A compact, economic scrubber to improve farm biogas upgrading systems

David Benizri, Nicolas Dietrich, Pierre Labeyrie, Gilles Hébrard

▶ **To cite this version:**

David Benizri, Nicolas Dietrich, Pierre Labeyrie, Gilles Hébrard. A compact, economic scrubber to improve farm biogas upgrading systems. Separation and Purification Technology, 2019, 219, pp.169-179. ⟨10.1016/j.seppur.2019.02.054⟩. ⟨hal-02158075⟩

HAL Id: hal-02158075

https://insa-toulouse.hal.science/hal-02158075v1

Submitted on 17 Jun 2019

HAL is a multi-disciplinary open access archive for the deposit and dissemination of scientific research documents, whether they are published or not. The documents may come from teaching and research institutions in France or abroad, or from public or private research centers.

L'archive ouverte pluridisciplinaire **HAL**, est destinée au dépôt et à la diffusion de documents scientifiques de niveau recherche, publiés ou non, émanant des établissements d'enseignement et de recherche français ou étrangers, des laboratoires publics ou privés.

HAL Authorization

A compact, economic scrubber to improve farm biogas upgrading systems

Benizri David[a], Dietrich Nicolas[a], Labeyrie Pierre[b], Hébrard Gilles[a]

[a] *Université de Toulouse; INSA, LISBP, 135 Av. de Rangueil, F-31077 Toulouse, France INRA UMR792, Ingénierie des Systèmes Biologiques et des Procédés, F-31400 Toulouse, France CNRS UMR 5504, Ingénierie des Systèmes Biologiques et des Procédés, F-31400 Toulouse, France*

[b] *ARIA ENERGIES, Z.A. de Baluffet,50/58 chemin de Baluffet, 31300 TOULOUSE*

Abstract

This paper presents a new biogas upgrading technology with its theoretical and experimental study and an application at farm scale. This process is designed for flows of raw biogas up to 50 Nm^3/h (55% CH_4 and 45% CO_2). The upgrading system includes a physical absorption of CO_2 at 7-10 bars in water and desorption at atmospheric pressure. First, the authors improved the traditional bottom column design to avoid usual formation of biogas bubble and leaks. As a second technological breakthrough, process water was successfully recycled using a static mixer to enhance CO_2 desorption from the water. Finally, the scrubbing system is entirely characterized; carbon dioxide absorption into the column is modeled thanks to the transfer unit height (HTU_{OG}) and the number of gas transfer units (NTU_{OG}); desorption step of CO_2 is performed into the static mixer at atmospheric pressure and modeled. Experiments with this new scrubber were conducted in farm with raw biogas; inlet flow rates ranged between 15.6 and 42 Nm^3/h. Upgraded biogas up to 77% (Q_G=40.7 Nm^3/h and Q_L=8.243m^3/h and P=7.924 bar and T=285K) is possible with good absorption efficiency (57.5%) and high methane recovery ratio (94%) and low power consumption (0.26 kWh/Nm^3).

Through the comparative analysis of the experimental results with the modelling proposed, authors are providing good references to evaluate this simple and cheap compact technology on a real farm biogas plant and its potential for fuel combustion engines.

Keywords: Anaerobic digestion, Biogas upgrading, Carbon dioxide, Methane, Water scrubber, Mass transfer

1. Introduction

To figure out energy issues in rural areas of the world, biogas is a suitable and alternative solution which is powerful and clean as shown in the objective review conducted by Holm-Nielsen et al. [1]. The raw biogas produced from the simplest farm plant is a mixture of carbon dioxide (35-50 per-cent vol.), hydrogen sulfide (500-2000 ppm) and methane (50-65 per-cent vol.) and it is saturated with water vapor. Biogas is obtained by anaerobic digestion of organic matter, a substrate coming from the food industry, agricultural wastes and cattle. As it is produced from waste of human activity, biogas is available in every part of the world. On farms, development of the biogas can be promoted by the development of new and efficient technologies. Biogas can be either burned in combined heat and power engines or upgraded by separating the components of high added value such as natural gas and pure carbon dioxide. Several applications of scrubbers have been studied theoretically by Mc-Nulty [2], and have already been applied for biogas upgrading in many countries at flow ranges higher than 100 Nm^3/h.

Previous research works in this area have highlighted several advantages of developing biogas upgrading with High Pressure Water Scrubbing (HPWS): Bauer et al. [3] and Ryckebosch et al. [4] consider it as a very advantageous solution for saving energy. It is also assumed that the solvent used and the compactness offered make it very environmentally friendly. Several studies of Life Cycle Assessment (LCA) have focused on HPWS technology. Overall, they show that upgrading biogas leads to better environmental impact (Pöschl et al. [5]) than using a combined heat and power generator. Pöschl et al. [5] compared HPWS to very recent technologies such as BABIU (Bottom Ash for BIogas Upgrading) or AwR (Alkali with Regeneration) which use carbon mineralization and its storage in solid form. As concluded by Starr et al. [6], HPWS is a low impact technology compared to cryogenics, hollow fiber membrane permeation, chemical absorption and Pressure Swing Adsorption (PSA). Considering HPWS, they also concluded that, if CO_2 storage is possible the Global Warming Potential (GWP) result is negative. Fresh water is generally used as the solvent in HPWS but it is expensive when only drinking water is available. Recycled water has been used as a common and economical solution. However, the necessary step of desorption has often

implied an air stripping scrubber and the system is considered as inconvenient nowadays. It is believed to prevent production of CO_2 and, according to Bauer et al. [3] and Kohl and Nielsen [7], it leads to bacterial contamination, sulfur oxidation and corrosion. Also, it adds undesired O_2 and N_2 to the CH_4 output. To conclude about water recycling, some improvement would be desirable in the way to regenerate water.

The range of flows investigated in this study (from 0-50 Nm^3/h for our HPWS) concerns small biogas productions. White *et al.* [8] showed it was cost efficient to sell electric energy from biogas combustion at such scale. However technologies are not affordable for biogas upgrading which is more profitable nowadays as pointed out by Bauer et al [3]. This throughput order is still being investigated *e.g.* by Lantelä et al. [9]. On the other hand, state of the art reports on the scientific literature ([9], [10],) and industry ([7]) present a wide range of HPWS process reaching efficiency and operational cost effectiveness, although compactness has not been considered yet for small gas flow rates.

In the literature, Rasi et al [11], Lantelä et al. [9] and Chandra et al. [12] are developing new technologies and automation of the HPWS process. Their studies have led to an experimental validation based on the methane volumetric content in the upgraded biogas. CO_2 mass balance is sometimes also calculated. A mass balance on the gas phase could be more suitable to appreciate the HPWS efficiency than the solely methane quality achieved. However it is not sufficient when issues appear, such as high dissolution of methane. A second mass balance on the liquid phase has to be performed. Personn [13] reviewed methane leaks in industrial biogas scrubbers and compared real operational data with constructor guarantees. In one case, up to 18% of the incoming methane was lost. Their work highlighted the need for more accurate measurements to characterize such losses. Saidi et al. [14] worked recently on HPWS adapted to low biogas flowrates, showing the capability to use partially upgraded biogas for fuel combustion engines. Maximum power was achieved at a CO_2 fraction of 25%. However their modelling approach didn't take into account the possible

dissolution of methane in water at the pressure under test.

The aim of our study is to furnish a new upgrading system for biogas handling at low cost, low environmental impact and low biogas flow rate (up to 50 Nm3/h) with no leaks. To meet this goal, the paper deals with new design, development and improvement of HPWS technology convenient for low gas flowrate and useful for fuel combustion engines.

First, the design step is precisely detailed with a conventional scrubber design method. Then a recent patent (Hébrard et al. [15]) is studied, in which the column is improved to reduce the methane leak observed at the CO_2 exhaust. Finally a patented method of desorption (Hébrard [16]) is presented and modeled. It consists of adjoining a static mixer to avoid an air stripped packing column as the desorption step. These innovations are majors as they address two main problems of HPWS. Indeed, they reduce energy consumption, air injection and methane loss during operation.

2. Theoretical design of the HPWS process

The following paragraph will present the Flow-sheet adopted to design the HPWS process; also will be presented the scientific approaches used to design the absorption step occurring into the packed column under pressure and then the desorption step performed into the static mixer and the long pipe.

2.1. Process Flow-sheet

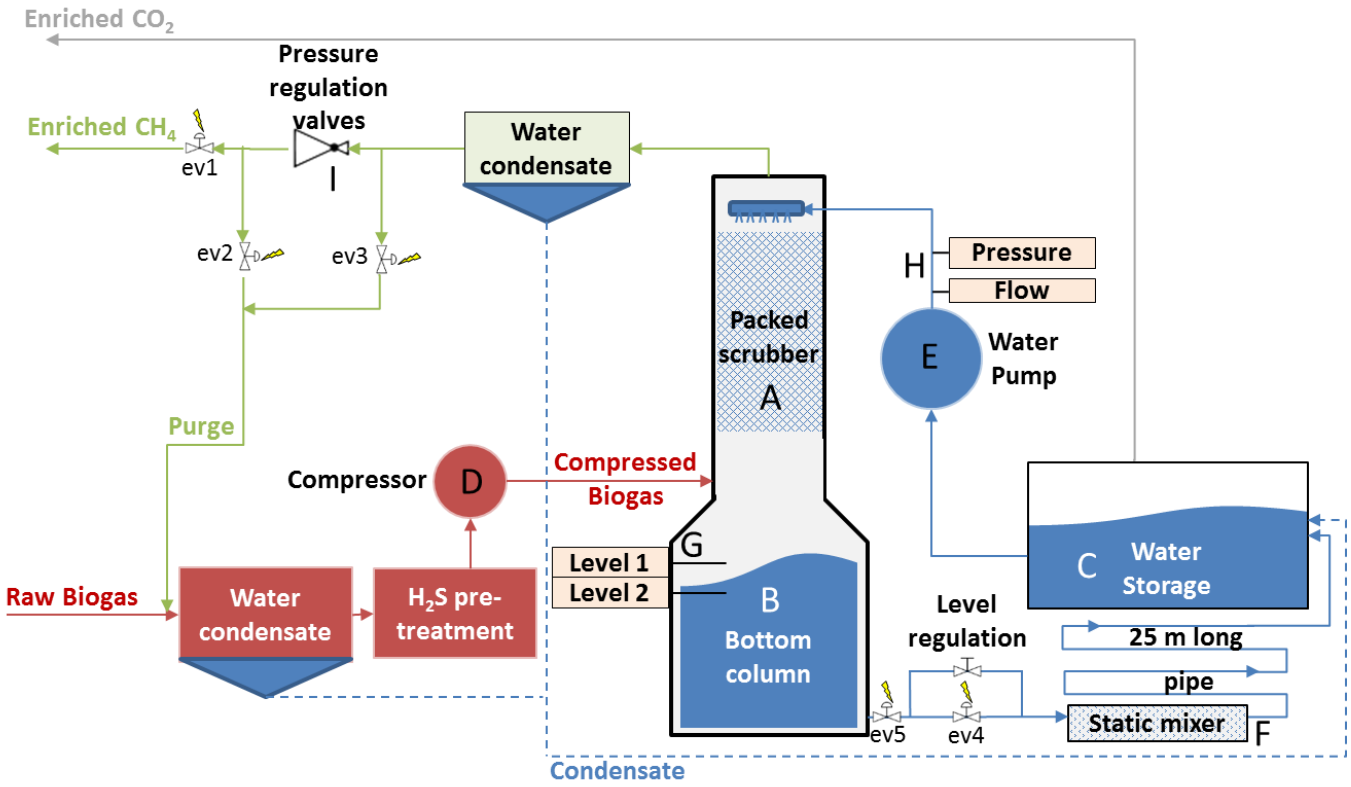

Figure 1 : Flow diagram of process integrated on farm

Figure 1 presents the main flows in the process. Raw biogas was admitted from an anaerobic digester. It was first pretreated to avoid liquid water and H_2S over concentration (≤ 300 ppm). This protected the compressor and equipment from corrosion. Biogas was compressed and fed into the packed scrubber where CH_4 was concentrated into the gas phase and CO_2 was transferred to the liquid phase. Methane was recovered at the top of the column at 7 bars through a pressure regulation valve. The water is injected at the top of the column thanks to a water pump via a perforated

tube as sparger. At the bottom of the column the saturated water is then released at atmospheric pressure by a valve. After each experimental operating period which can vary from 1 to 5 hours, the column was purged: then the column pressure was brought to atmospheric pressure and the depressurized gas was recycled to the treatment and compression equipment in order to protect them from corrosion by static biogas. Figure 1 also illustrates how water was recirculated from the absorption column to desorption devices during the operating period. A level regulation system placed in the column feet ensured that water was kept at 1 m above the column water outlet. Two vibrating level switches were used for that. After the release valve, the water was led through the static mixer and circulated in a 25 m long pipe in order to enhance gas desorption and to promote the coalescence of bubbles provided. Then the water was re-injected into the absorption column after the previously absorbed CO_2 had been released into the storage tank through the exhaust gas outlet. The major electricity consumers of the process were the biogas compressor and the water pump.

2.2. Absorption step

The absorption step was designed in two phases. First, was calculated the upper part of the packing column where CO_2 absorption occurs. The bottom column was also improved to ensure low biogas leakage. Two specific parameters E_{CO_2} and R_{CH_4} were defined to meet the upgrading goal. They respectively answered the questions “How much CO_2 has been transferred?” and “How much CH_4 has been lost?”. In fact, although the methane Henry constant predicted low methane absorption in water, methane gas flow depletion was still observed between injection and production. The parameters were defined as:

$$\boldsymbol{E_{CO_2}} = \frac{y_{CO_2\ in} - y_{CO_2\ out}}{y_{CO_2\ in}}$$

Equation 1

$$\boldsymbol{R_{CH_4}} = \frac{\dot{n}_{CH_4\ out}}{\dot{n}_{CH_4\ in}}$$

Equation 2

R_{CH_4} = 1 corresponds to the special case where only CO_2 is absorbed and CH_4 is considered as inert. For the sake of simplicity, the theory was based on this case, and the value of the E_{CO_2} parameter of the model diminished when R_{CH_4} was lower than 1.

The first step in designing a scrubber is to calculate the molar mass of solvent necessary to reach the CO_2 absorption goal.

For a dilute solution, in contact with a gas mixture where CO_2 is the solute to be absorbed, the equilibrium of phase fugacity follows the Henry's law, where y is the gas phase molar ratio of gas of interest and x is the liquid phase molar ratio.

$$y_{CO_2} = m \cdot x_{CO_2}$$

Equation 3

m is the sharing coefficient of the gas between the gas and liquid phases. It was calculated using the Henry's constant and assuming activities and fugacity coefficients to be equal to 1.

$$m = \frac{H_{CO_2}}{P}$$

Equation 4

The molecular flows of gas and liquid for absorption have to respect:

$$A = \frac{L}{m.G}$$

Equation 5

A is the absorption ratio which must be greater than one to fulfill the equilibrium law.

Assuming that y_{CO_2} can vary along the column height, the CO_2 absorption balance was written through the non-transferring component (methane).

$$Yi = \frac{m \cdot Xi}{1 + Xi(1 - m)}$$

Equation 6

Where liquid Xi and gas Yi molar ratio are relative to non-transferring components and expressed as:

$$Y_i = \frac{y_i}{1 - y_i}$$

$$X_i = \frac{x_i}{1 - x_i}$$

This allowed the minimal solvent flow L_i to be found, for given (X_{out}, Y_{in}) which are bottom conditions for the non-transferring gas, i.e. methane. By choosing an absorption ratio A equal to 1.4, this minimal molar flow was rose by 40% to ensure the performance of absorption, so that:

$$L_i = 1.4 \cdot G_i \cdot \frac{Y_{in} - Y_{out}}{X_{out} - X_{in}}$$

Equation 7

Once the thermodynamic conditions are satisfied by a sufficient liquid flow, the gas and liquid have to flow through the packed column. In fact, too much gas or liquid can induce a large pressure drop or flooding. Considering volumetric flows of gas and liquid, the following correlations between flows and column diameter was used.

$$X_{Flood} = \frac{L_M}{G_M} \cdot \sqrt{\frac{\rho_G}{\rho_L}}$$

Equation 8

When X_{Flood} was determined, an ordinate Y_{Flood} was given by using Sawitowski's correlation [17]. This ordinate Y_{Flood} was then related to the maximum gas velocity without flooding ($U_{G_{Flood}}$) by:

$$Y_{Flood} = \frac{F}{g} \cdot \left(\frac{\rho_{H_2O}}{\rho_L}\right)^{0,2} \cdot \frac{\rho_G}{\rho_L} \cdot \left(\frac{\mu_L}{\mu_{H_2O}}\right)^{0,2} \cdot U_{G_{Flood}}^2$$

Equation 9

The maximum gas velocity possible without flooding provided the working velocity U_G thanks to a security factor:

$$U_G = 0.65 \cdot U_{G_{Flood}}$$

Equation 10

Lastly, the required column diameter was calculated respecting all the conditions employed so far:

$$Dc = \sqrt{\frac{4 \cdot Q_G}{\pi \cdot U_G}}$$

Equation 1

The design method has to be performed under a steady state operation to reach such an absorption rate. It was carried out following conventional mass transfer theory

reported by Roustan [18] where the number of transfer units and height of transfer units were considered.

To specify the column height Z_C, the transfer unit height, HUT_{OG}, and the number of transfer units, NUT_{OG}, are commonly used.

$$Z_C = HTU_{OG} \cdot NTU_{OG}$$

Equation 2

The height of a transfer unit was calculated from:

$$HTU_{OG} = \frac{Q_G}{K_G \cdot a^0 \cdot \Omega}$$

Equation 3

The global mass transfer coefficient K_G for gas was obtained by considering double film theory of Whitman [19] where both gas and liquid phases contributed to the mass transfer. For a given packing column, the global transfer followed Onda et al. [20] correlation (equation 15) involving gas and liquid films transfer coefficients $k_G{}^0$ and $k_L{}^0$:

$$\frac{1}{K_G{}^0} = \frac{1}{k_G{}^0} + \frac{m}{k_L{}^0}$$

Equation 4

$$k_L{}^0 = k_L \cdot \frac{\rho_L}{M}$$

Equation 5

$$k_L = 5.1.10^{-3} \cdot \left(a^* \cdot d_p\right)^{-0.27} \cdot \left(\frac{a^0}{a^*}\right)^{-\frac{2}{3}} \cdot Re_L{}^{\frac{2}{3}} \cdot Sc_L{}^{-\frac{1}{2}} \cdot \left(\frac{\rho_L}{\mu_L \cdot g}\right)^{-\frac{1}{3}}$$

Equation 6

All other terms could be explained with correlations adopted by Onda et al. [20], which are reliable for random packing (cf Appendix B.).

$$k_G{}^0 = k_G \cdot \frac{P}{R \cdot T}$$

Equation 7

The gas mass transfer coefficient k_G was expressed with the following Sherwood number correlation.

$$k_G = Sh_G \cdot \frac{D_G}{d_{eq}}$$

Equation 8

$$Sh_G = 5.23 \cdot (a^* \cdot d_p)^{-0.27} \, {Re_G}^{0.7} \, {Sc_G}^{\frac{1}{3}}$$

Equation 9

The number of transfer units required NUT_{OG} was evaluated with E_{CO_2} and A by:

$$NUT_{OG} = \frac{A}{A-1} \ln\left(\frac{A - E_{CO_2}}{A(1 - E_{CO_2})}\right)$$

Equation 20

The table 1 reports the fixed parameters for the column design as the inlet flow of biogas, a selected absorption ratio A and a selected absorption efficiency E_{CO_2} ; from this considered values, the column height Zc , column diameter Dc and mass transfer parameters are calculated and reported in table 2.

Parameter	Value	Unit
Q_G	40	Nm^3/h
P	7	bar
A	1.4	-
E_{CO_2}	0.95	-

Table 1 : Chosen values for the scrubber design

Parameter	Value	Unit
Q_L	10	m^3/h
D_C	0.25	m
HTU_{OG}	0.5	m
NTU_{OG}	5.94	-
Z_C	2.98	m

Table 2 : Calculated mass transfer parameters of the packed column

We can see in Table 2 that Zc=2.98 m; a 3m height packing column has been considered to make our scrubber.

To complete the absorption step design, bottom column diameter must be calculated; we did it in order to reduce biogas leaks. A method developed to limit the loss of methane and patented by Hébrard et al. [15] was used here. A bottom part twice as large as the column part diminished the liquid velocity, thus enabling smaller inclusions to be entrained by the liquid down-flow. The study was conducted firstly by simulation. To avoid any bubble entrainment, the liquid velocity has to be 1.3 times lower than the ascension velocity of a bubble $U_{b_{mean}}$.

$$U_{b_{mean}} \geq 1.3\, U_{L_{mean}} = 1.3 \cdot \frac{4 \cdot \mathrm{Q}_L}{\pi \cdot {D_{bottom}}^2}$$

Equation 1

For a given velocity of liquid, it is possible to calculate the related bubble diameter kept in the flow. if $d_{b_{mean}} \leq 0.7$ mm as specified by Treybal [21], Stokes equations were applied.

$$d_{b_{mean}} = \sqrt{\frac{18 \cdot U_{b_{mean}} \cdot \mu_L}{(\rho_L - \rho_G) \cdot \mathrm{g}}}$$

Equation 2

Otherwise, the bubble ascension velocity was expressed thanks to the Schiller and Neumann correlation of the drag coefficient involving the Reynolds number. d_b was initialized at 3.10^{-4} m.

$$Re_{b_{mean}} = \frac{\rho_L \cdot (1.3 \cdot U_L) \cdot d_{b_{mean}}}{\mu_L}$$

Equation 3

$$C_D = \frac{24}{Re_{b_{mean}}} \cdot (1 + 0{,}15 \cdot {Re_{b_{mean}}}^{0.687})$$

Equation 4

$$d_{b_{mean}} = \frac{6}{2} \cdot \frac{{U_{b_{mean}}}^2 \cdot C_D \cdot \mu_L}{(\rho_L - \rho_G) \cdot \mathrm{g}}$$

Equation 5

These calculations were iterated until $Re_{b_{mean}}$ and $d_{b_{mean}}$ were stable. Table 3 shows the results of the calculations for two common diameters and the designed liquid flow.

D_{bottom} [m]	Q_L [m^3/h]	d_b [m]	Re_b
0.3	10	0.000889	34.886
0.6	10	0.000154	1.959

Table 3 : Maximum bubble diameter kept in liquid flow versus bottom column diameter

From this approach a bottom column diameter of 0.5m has been considered to make our scrubber.

2.3. Desorption step

It was decided to recycle the water with a new regeneration method using a static mixer followed by a long pipe and a storage tank. This apparatus provided various

benefits that had been predicted theoretically. On the one hand, the static-mixer was considered as a necessary precursor for changing the phase of the CO_2, from an over-saturated liquid phase to a concentrated gas phase. This phenomenon was modeled successfully.

The static mixer was designed as described in the thesis of Heyouni [22] where several static mixers were studied. First, the power dissipation was evaluated. For Fisher et al. [23], Zhou [24] and Heyouni [22], the power dissipation in a static mixer was:

$$\frac{P_{dis}}{\Sigma} = \frac{\Delta P \cdot Q_L}{\rho_L \cdot \epsilon_{SM} \cdot (1 - \epsilon_G) \cdot V_{SM}}$$

Equation 6

This information gave us the Sauter equivalent bubble diameter d_{bs} which followed the law of Hinze in forced convection and under turbulent conditions (typical conditions of statics mixers) according to Roustan [18].

$$d_{bs} = \alpha \cdot \left(\frac{\sigma}{\rho}\right)^{0.6} \cdot \left(\frac{P_{dis}}{\Sigma}\right)^{0.4}$$

Equation 7

$$\alpha = \frac{1}{2} \cdot We_{crit}{}^{0.6}$$

Equation 8

$$We_{crit} = \frac{\rho \cdot U_{G_{crit}} \cdot d_b}{\sigma}$$

Equation 9

We_{crit} was the critical Weber number that gave a maximal size of bubble for critical conditions of flow. Andreussi et al. [25] obtained α = 1.1 for bubbles in horizontal pipes for an air/water system and this value was applied in our case.

On the other hand, the static mixer enhanced the rate of the transfer from a liquid phase to a gas phase when they were not equilibrated.

According to Zhou [24] the oxygen volumetric mass transfer coefficient $K_L a_{O_2}$ for a Kenics® static mixer can be approximated by:

$$\mathrm{K_L a_{O_2}} = 4.56.10^{-4}\left(\frac{P_{dis}}{\epsilon_{SM} \cdot (1 - \epsilon_G) \cdot V_{SM}}\right)^{0.68}$$

Equation 30

As the present work involved biogas, the volumetric mass transfer coefficient value was needed for CO_2. According to Roustan [18], in a sphere when poorly soluble compounds are considered, transfer coefficients are proportional to the diffusion constant $D_{A\to B}$. This gives

$$\mathrm{K_L a_{CO_2}} = \mathrm{K_L a_{O_2}} \cdot \frac{D_{CO_2\to water}}{D_{O_2\to water}}$$

Equation 1

where $D_{A\to B}$ constant were evaluated in operational condition with Wilk and Chang's correlation [26]. Considering the benefits of the static-mixer mentioned previously, it was possible to determine the mass balance of this apparatus. Only the CO_2 in the liquid phase was considered.

Various mass balances have been used to model gas-liquid contact devices. As Devos [27] concluded, Kenics® static-mixers were well modeled using a tubular flow reactor (only 20% of dispersion of the residence time distribution around the reactor piston response to a scale perturbation), considering the previous $\mathrm{K_L a_{CO_2}}$ coefficient.

$$\mathrm{C}_{out} = (\mathrm{C}_{in} - C^*)\exp(-\mathrm{K_L a_{CO_2}} \cdot \tau) + C^*$$

Equation 2

Finally the water and the desorbed gas were sent to the separation tank via a pipe. Another mass balance was carried out to predict CO_2 concentration in the liquid phase. The 25 m long pipe was modeled considering a stratified flow with 70% of void fraction and a tubular reactor with a driving force explained by a logarithmic mean due to the plug flow. The stratified flow was chosen after observation, and allowed the mass transfer coefficient $\mathrm{K_{L_{pip}}}$ to be attained. Transfer was controlled by the high turbulence of the gas over the liquid surface S [m^2] according to Roustan [18] with further information given by Calmel and Magnaudet [28].

$$\mathrm{C}_{out} = (\mathrm{C}_{in} - C^*)\exp\left(-\mathrm{K_{L_{pip}}} \cdot \frac{S}{Q_L}\right) + C^*$$

Equation 3

Kenics ® static-mixer			Horizontal Pipe		
L	m	0.5	L	m	25
d	m	0.05	d	m	0.05
ϵ_{SM}	-	0.13	S	m^2	1.18
d_{bs}	m	1.13.10	$K_{L_{pip}}$	$m.s^{-1}$	$2.51.10^{-3}$
τ	s	0.36			
$K_L a_{CO_2}$	s^{-1}	0.239			
C_{in}	(mol/m^3)	116,22	C_{in}	(mol/m^3)	110
C_{out}	(mol/m^3)	110	C_{out}	(mol/m^3)	63

Table 4: Theoretical parameters of the desorption device

3. Material and Methods

3.1. Construction material description

The column was a tube of external diameter 30 cm and thickness 2 cm, so its internal diameter was slightly greater than the designed diameter in order to complete upgrading of gas flows from 30 to 50 Nm^3/h, showing an internal volume of 300 L. However, the experiments were conducted with an inlet gas flow between 15.6 and 42 Nm^3/h. The upper part of the column was made of polyethylene. The bottom column was made of iron metal and was protected from corrosion by inert paint. It had 0.5m in diameter and an internal volume of 400 L. Water tubes were made of stainless steel and PVC. All gas tubes were made of stainless steel. The whole system could withstand 16 bars. The desorption tank was made of polyethylene, had a capacity of 1200 L and was not resistant to high pressure.

3.2. Automation and power equipment

Ensuring good automation of the scrubber was a key issue in this work. It reduced energy losses, avoided risks of misuse and allowed for use of a remote control as protection in case of blast. The process was stable and produced upgraded methane after 5 to 10 min of operation. This goal was reached by using frequency drivers for pump and compressor, ATEX electric- valves, level sensors, water flow and pressure sensors. The system was then controlled by an industrial computer acting as the human-machine interface.

3.3. Equipments

The tank for storing the recycled water was integrated around the bottom column. The different equipments used are reported into tables 5 and 6.

Equipment	Pump	Compressor
Type	Salmson MultiV800	Mauguières MRL100-10
Characteristics	20 m^3/h at 10 bars	78 Nm^3/h - 10 bars
Control	Frequency driven	Frequency driven

Table 5: Power equipment

Equipment	Gas valves	Liquid valves	Level sensor
Type Characteristics	Asco serie NF WSNF	ASCO serie 210 230Volts	Bürkert level switch 8111

Table 6 : Control equipment

The pumps, compressor, methane recovery system, carbon dioxide recovery system and pipes were contained in a 2 square meters. Hébrard patent's [16] concerns the use of a static mixer to make the apparatus smaller and to ensure good desorption despite the use of a stripping column.

3.4. Random Packing

Figure 2 : Raschig Super Ring® example

The most important specifications for random packing are the free space (ϵ) it offers to circulation of both currents, and the area of contact created (a). In the case of this demonstrator, an innovative packing from Raschig GMBH (figure 2), called Super Ring ®, was implemented to reach the design flow rate. Its characteristics are reported in table 7.

Packing Type [material]	d [m]	a* [m^2/m^3]	ϵ_G
Raschig Super Ring [PP]	0.05	250	0.9

Table 7 : Packing characteristics

3.5. Analysis material

Particular attention was paid to ensuring good gas analysis.

Water vapor was eliminated from the gas using a Peltier cooler (Herrmann Moritz) and a 200 micrometer filter. Gas flow and pressure were regulated before drying and analysis to ensure samples of the best possible quality.

Nowadays, the error of infrared analyzers is less than 0.02 %. The equipment owned

by the laboratory is specific to biogas. It is called “Bio-basic” and was procured from the “Gruter et Marchand” company. It analyses the CH_4, and CO_2compounds with an IR sensor, and electrochemical cells complete the analysis of the H_2, O_2 and H_2S. Pressure was measured by an Endress+Hauser sensor (Cerabar TP31) having 0.3 % full scale error, *i.e.* 3kPa.

To characterize the behavior of the scrubber, liquid control and analysis were also conducted. It was essential to know the acidity if the evolution of the water saturation by carbon dioxide was to be followed. A pH meter (HACH - HQ40D multi) calibrated at each trial took samples every 30 seconds during the whole trial. It gave the pH and temperature of the water.

3.6. Experimental methodology

The first step of the study was to collect the data generated when the HPWS process was running. This step is described in 3.7 and used equipments are described in 3.5. The second step was the analysis of data.

Temperature as the pH of the water were measured in the desorption tank. Raschig Super ring packing was used for all trials. Gas flow, water flow and temperature were investigated throughout the study. An experiment lasted for three to five hours. Inlet and outlet biogas were analyzed to calculate the CO_2 absorption efficiencies and methane loss for different operating conditions. All the upgraded biogas was recycled to the anaerobic digestion plant.

3.7. Typical aggregated results

Figure 3 presents a typical case of process management and data gathered simultaneously. The process began after a waiting period of 30 min. First, the pressure rose as compressor was running and when 6.5 bars were reached, liquid flow was injected. For the first ten minutes, parameters fluctuate because all the valves had a specific regulated position. On the figure 3, the first steady state was reached at 00:45. As pressure was higher than expected, the pressure regulation valve was activated at 01:12 and pressure decreased. Pressure and flow variations were the result

of the process control by an operator. When a desired condition was reached, a result was taken into consideration after 10 min of stable pressure and flows. To make it practical, data were considered only once the steady state was achieved. For example, in figure 3, it was reached at 02:10. This led to complete and reliable experimental results. All these reliable points are presented later in Table 9 for 40 experiments.

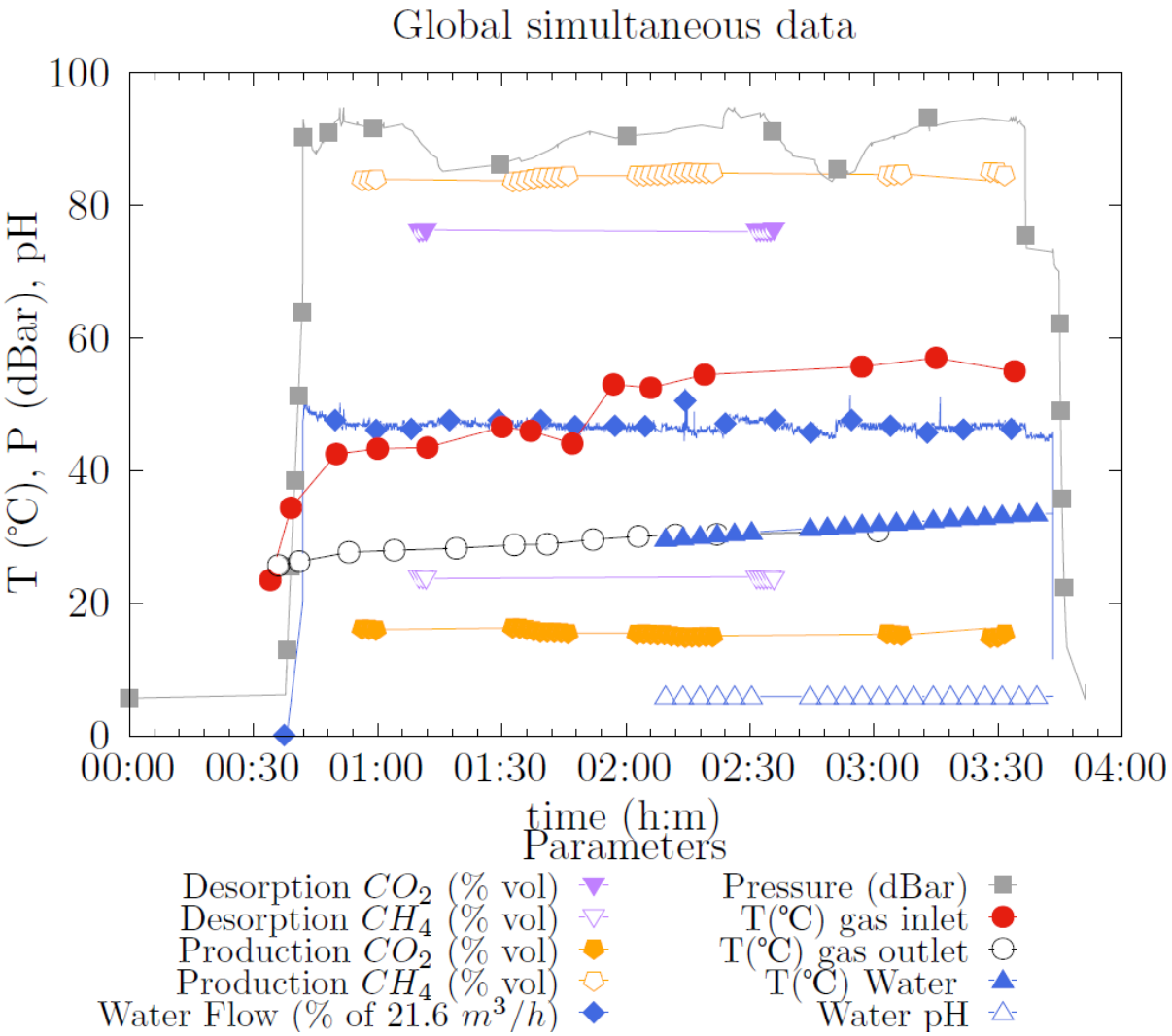

Figure 3 : Example of collected data measurements

4. Experimental results

4.1. Evaluations of heat transferred

During compression, mechanical movements heated parts of the compressor but also

the gas, leading to an increase in the compressed gas temperature. Considering the real transformation from the original state of the biogas (1.03 bar, 308K) to the hot compressed biogas (9 bars, 323.15K), the biogas shows a net gain of heat power of 0.1 kW during compression. The gas flow in the scrubber was totally saturated and condensates could be observed at the inlet and at the outlet of the column. Water vapor content was considered to be equal to the saturating vapor pressure for the scrubbing conditions. While circulating through the scrubber, gas cooled progressively and reached the water inlet temperature. At the same time a small amount of water was transferred to the gas. This heat transfer necessary to cool the gas and to evaporate water was calculated on the basis of experimental data. It represented 0.2 kW of power transferred to the water from the gas during operation. Water took a part of the gas inlet heat and was cooled by a small amount of evaporation. This whole power corresponded to 0.2 kW, so water temperature increased. Water was also pumped which constituted another heat source. By measuring the water temperature variation during the process operation, it was calculated that the total amount of heat transferred to the water represented a net power of 2.08 kW.

4.2. pH evolutions

Dissolution of acid gases such as hydrogen sulfide (H_2S and CO_2) caused the water acidity to increase. This provided a good parameter to study whether CO_2 was accumulating in the recycled water. As can be seen in figure 4, in the absence of H_2S in the inlet biogas and at a constant temperature of 292.15 K, pH in recycled water often stabilized between 5.8 and 6 which represent equilibrium in water with 78.7 to 70% of CO_2 and 21.7 to 30% of HCO_3^-; however miss the CO_2 concentration measurement into the liquid. As there was no evolution, it was considered that an equilibrium between absorption and desorption had been reached. This confirmed that desorption device was extracting the gas; otherwise accumulation of dissolved CO_2 would have provoked an acidification of the recycled water.

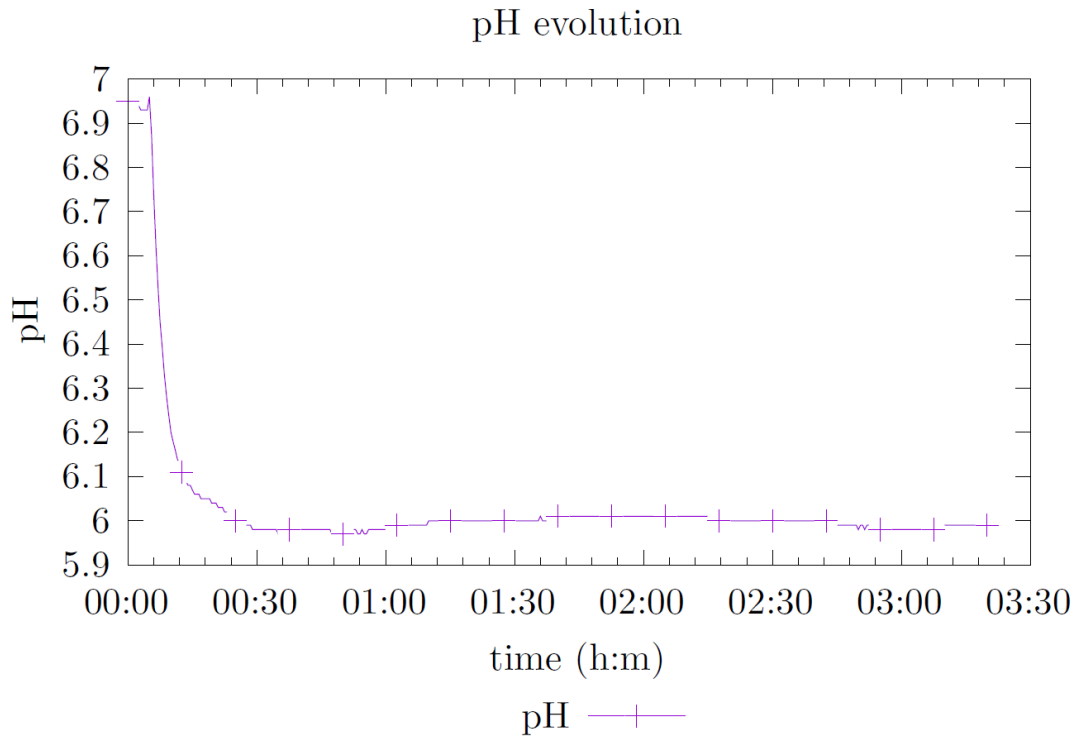

Figure 4 : pH stabilization

4.3. Results of bottom column improvements

Developed in part 2 and in the second patent of Hébrard et al. [15], the calculation of the bubble retention and formation in the bottom column was confronted with experimental imaging to validate whether the phenomenon of biogas retention had been overcome or not. An image frame shows very clear improvements on this important point. A retro-lighted CCD camera (Photron Fastcam SA3, 120 K: 2000 frames per seconds (fps) at 1024 x 1024 pixel) has been used, with imaging frequency of 1000 fps (figure 5) and 3000 fps (figure 6). Figure 5, related to a 0.25 m bottom column diameter, shows gas retention of 2.5% with a jet of bubbles having size from 0.15 mm to 0.8 mm. Figure 6, related to a 0.5 m bottom column diameter, shows no bubbles in accordance with predicted diameter reported in table 3. However, the camera could detect only bubbles larger than 0.1 mm because of the resolution limits of the camera and its lens. This improvement has been patented by Hébrard et al. [15] and constitutes a second innovation of this work.

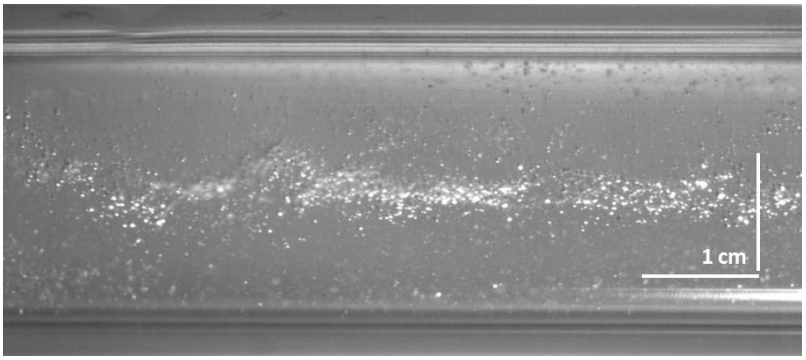

Figure 5 : Bubble leaking at the liquid outlet with a 0.25 m bottom column

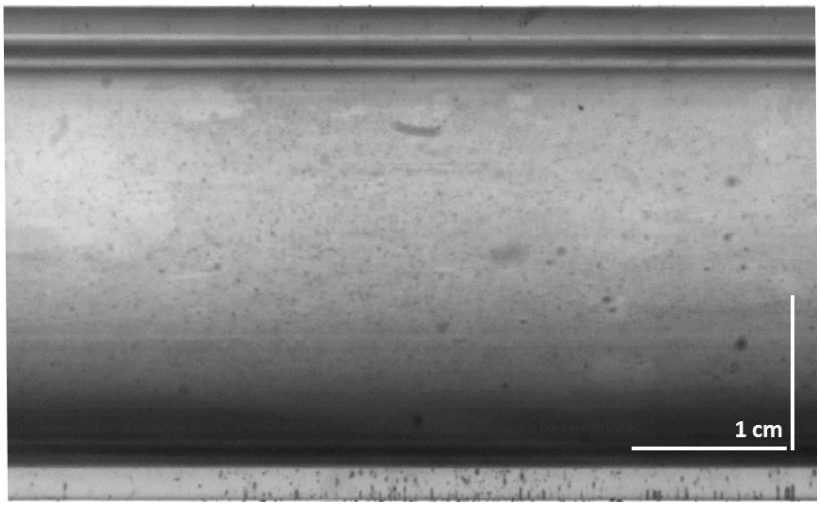

Figure 6 : Absence of bubble leaking at the liquid outlet with a 0.50 m bottom column

4.4. Power consumption of the experimental system

The compressor electricity consumption was 2.5kW. Such a polytropic transformation needs 1.24 kW, so a polytropic yield of 49% can be deduced which is very low for this type of compression. Measurements made during process operation were taken directly on the electric grid for HPWS and Fridge set-up for cooling water. The results are presented in table 8.

System	Value	Unit
HPWS	6.8	kW
Fridge	3.5	kW

Table 8 : Net consumption of electricity of the whole process

Regarding the energy consumption per Nm^3 of raw biogas, HPWS consumed 0.19

kWh/Nm^3. In other trials the water was cooled using a refrigerator (Fridge in table 8) to maintain the temperature level suitable for absorption. This led the energy consumption to 0.26 kWh/Nm^3.

4.5. Table of results

Table 9 reports all the data collected during 40 experiments and obtained with the absorption system.

	Q_L(m^3/h)	Q_G(Nm^3/h)	P_{CO_2}(bars)	P_{CH_4}(bars)	T_L(K)	E_{CO_2}(%)	R_{CH_4}(%)	CH_4 (%)
1	10	20.7	3.771	5.2	299.5	74	77.5	84.3
2	9.979	16.7	3.514	4.544	288.2	73.7	78.4	84.7
3	5	16	3.371	5.072	292.9	72.1	80.9	83
4	7.5	15.8	3.173	4.774	292.9	71.4	78.3	83
5	5	17.3	3.729	5.142	301.6	71.2	88.2	82.4
6	10	21.2	3.52	4.854	300.1	70.8	85.3	82.9
7	9.989	23.4	3.622	4.732	288.4	67.2	85	82.6
8	9.841	30.2	3.544	4.629	288.9	58.8	88.4	79.0
9	9.19	41.9	3.609	5.003	284.6	58.2	92.1	71.9
10	10	24.3	2.744	3.689	301.1	58.1	85.3	77.9
11	9.283	38.5	3.438	4.818	283.3	57.7	89.7	73.7
12	8.243	40.7	3.557	4.367	285.2	57.5	93.9	77
13	10	25	2.847	3.601	301.1	57.5	82.3	71.8
14	9.439	35.8	3.24	4.275	289.7	54.5	93	73.4
15	9.939	37.6	3.599	4.944	289.4	54.1	88.5	74.4
16	9.374	40.1	3.232	4.027	288.4	53.5	95.5	66.0
17	9.306	38.3	3.143	4.138	281.9	53.5	97	72.0
18	8.535	41.6	3.453	4.449	287.2	53.2	95.4	72.3
19	9.83	38.2	3.548	4.634	289.6	52	92.5	76.6
20	8.783	39.9	3.301	4.31	290.7	51.6	94.8	72.3
21	9.361	39.5	3.207	4.395	289.5	51.5	93.2	69.8
22	8.867	39.1	3.224	4.21	289.6	51	95.2	72.5
23	10	22.7	2.291	2.981	294.9	50.3	93.4	73.96
24	9.45	39.5	3.345	4.791	290.4	49.5	88.7	73.2
25	8.702	40.1	3.356	4.382	294.4	49.3	95.9	70.3
26	9.927	39.4	3.262	4.388	291.6	49.2	91.2	73.4
27	9.869	43.8	3.603	4.706	290.2	48.9	92.7	75.0
28	9.914	38.9	3.098	4.488	291.7	48.5	88.1	72.0
29	9.739	37.1	3.11	4.374	302.4	48.3	94.7	75.2
30	9.86	38.5	3.616	4.958	296.1	47.8	87.5	74.1
31	9.666	42.0	3.513	5.09	292.6	47.4	86.3	71.8
32	10.001	39.9	3.672	4.879	299.2	46.9	86.9	73.7
33	9.829	39.1	3.598	4.781	297.7	45.7	88.1	73.1
34	9.863	39.3	3.244	4.478	301.7	44.8	92.2	73.1

35	9.677	39.9	3.432	4.511	298.5	43.4	91.5	73.8
36	6.931	38.6	3.409	4.939	290.8	43.2	90.5	71.1
37	6.934	39.2	3.471	5.03	290	42.9	90.9	71.5
38	10.009	39.4	3.355	4.719	303.4	42	89.6	73.2
39	7.098	38.8	3.376	4.698	292.6	41.7	92.5	71.0
40	5.034	38.4	3.509	4.883	292.6	37.1	94.7	69.5

Table 9 : Experimental results at steady state of the packed column

As can be seen in Table 9, the applied gas flow varied from nominal calculations in 2.2 (40Nm^3/h) to a degraded flow of 15.8 Nm^3/h. Inlet flow of water was investigated from 5 to 10 m^3/h. As shown, the produced gas had a CH_4 concentration between 69.5 % and 84.3 % in volume. Two useful parameters that characterize carbon dioxide absorption (E_{CO_2}) and methane loss (R_{CH_4}) and that can varied inversely with operating parameters, have been estimated for each experiment and reported into the table 9. R_{CH_4} is an important parameter to characterize absorbers performance in biogas upgrading; it varies between 77% and 95.9% in this study. Regarding methane loss (R_{CH_4}), it can be painful for economic and environment so it is very important to master its variation.

4.6. Studies and analyse of global data

Figure 7 has been drawn to highlight the impact of the water flow on absorption column performance.

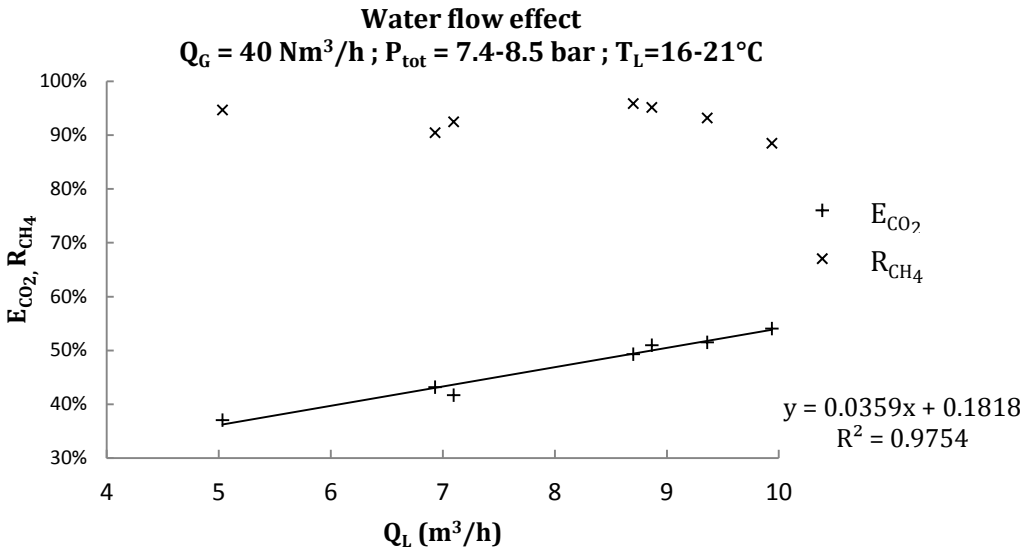

Figure 7 : Water flow effect on biogas upgrading

It can be seen that E_{CO_2} was clearly in relation with the flow of water. It confirms that absorption of CO_2 is successfully described by a linear relation with solvent flow (see equation 6). On the other hand, R_{CH_4} variation was not following a tendency and stayed high between 88.5% and 95.9%.

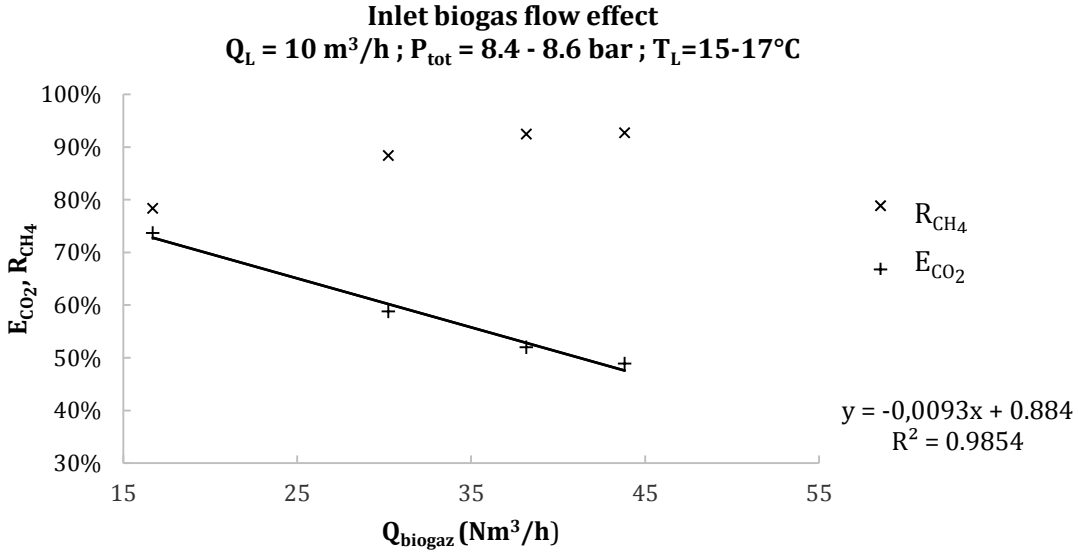

Figure 8 : Inlet biogas flow effect on biogas upgrading

Considering the impact of Q_G on absorption, the link between E_{CO_2} and the gas flow Q_G is nearly linear but inversely proportional as can be seen in figure 8.

This behavior fits to the theory of height of a transfer unit, which follows equations 12 and 13 rewritten as:

$$HTU_{OG} = \frac{Q_G}{K_G \cdot a^0 \cdot \Omega} = \frac{Zc}{NTU_{OG}}$$

Equation 34

As the real height of column Zc is invariant and Ω and a^0 are constant, the height of a unit of transfer increases with increasing gas flow. K_G also rises but slowly. Finally, increasing gas flow decreases the number of unit of transfer and lowers the efficiency E_{CO_2}. The methane recovery ratio, R_{CH_4} tended to be proportional in comparison to the gas flow.

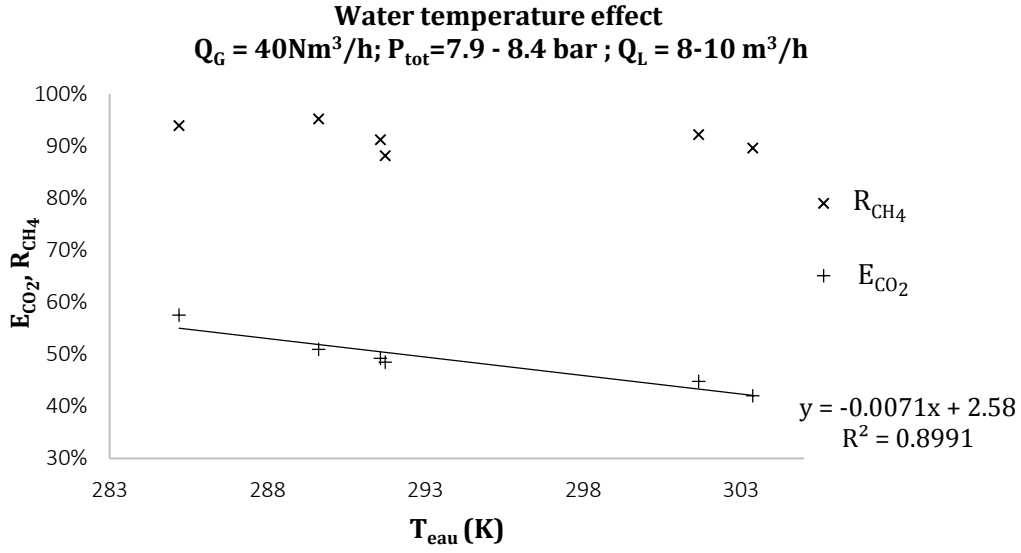

Figure 9 : Water temperature effect on biogas upgrading

The study of figure 9 clearly indicates that there is a proportional link between E_{CO_2} and temperature, which is also understandable because in Henry's law of dissolution, the equilibrium is assumed variant with temperature. Henry's law predicts that the

more the temperature is, the lower are the liquid molar fraction of carbon dioxide and so the absorption efficiency.

Both rates variation are in accordance with the theory used for design the apparatus. The greater are temperature, pressure and liquid flow, the greater is the absorption rate. Greater is biogas flowrate lower is carbon dioxide absorption efficiency and greater is methane recovery ratio. The recover methane ratio decreases when liquid flow increases. Considering these both rates, it is possible to select an optimal condition of work for high absorption rate and high recover methane with low power consumption. One optimum condition identified corresponds to the experiment number 12 : Q_G=40,7 Nm^3/h and Q_L=8.243 m^3/h and P=7.924 bar and T=285K with enriched biogas up to 77% of methane, with good absorption efficiency (57.5%) and with high methane recovery ratio (94%) and low power consumption (0.26 kWh/Nm^3).

4.7. CO_2 product quality

Although these results guaranteed a good CO_2 absorption and recovery of CH_4, constants of dissolution calculated from experiments were higher for methane (H_{CH_4}) than those previously taken into account by literature. Knowledge of the molar fraction in the biogas inlet, in the upgraded biogas outlet and in the CO_2 exhaust gas, was necessary to calculate the amount dissolved in water considering mass balances and pseudo-equilibrium for both molecules. H_{CH_4} and H_{CO_2} were then calculated with the most favorable conditions of mass transfer for both gases. For methane, the favorable conditions were the top of the column, with the higher methane partial pressure. For carbon dioxide, the inlet conditions were preferable. These conditions of partial pressure P_i, water temperature and the related calculated H_i constants are given in Table 10.

Step	P_i[kPa	T[K]	H_{CH_4}	H_{CO_2}	H_{CH_4} [MPa]	H_{CO_2} [MPa]
Top	445.5	298	2684	-	3970	-
Botto	309.1	298	-	896	-	169

Table 10 : Experimental Henry constants and literature Henry constants from Mao et al. [29] and Duan et al. [30] with

These results are extremely surprising as they prove that, on the one hand the methane concentration in water can exceed the theoretical maximum calculated using the Henry constant for pure water and single molecule. Is there an effect of gas mixture and water properties? On the other hand, carbon dioxide concentration in water was 5 times lower than it should be, so its transfer to water was not totally achieved. It may be explained considering that water has only been partially desorbed in regeneration system and so the potential of absorption has been lowered.

5. Discussion on performances of the system

The partial regeneration of water is proven with the stability of pH. Carbon dioxide did not accumulate too much in water. However, the dissolved CO_2 concentration in recycled water has not been determined.

When designing the process with the theoretical approach exposed in 2.2, initial carbon dioxide concentration has been considered null. Indeed, we have experimental efficiency of CO_2 absorption much lower (57.5%) than theoretically expected (95%) at the nominal flows (Q_G=40.7 Nm^3/h and Q_L=8.243m^3/h) and operating parameters (T=293,15K and P=7.924bar). It will be relevant to achieve the carbon dioxide desorption by cooling the static mixer and adding a void pump in order to maintain a stronger driving force and mass transfer.

So we show at the farm scale for low biogas flowrates, that upgrading biogas is relevant with good absorption efficiency (57.5%) and high methane recovery ratio (94%), and low power consumption (0.26 kWh/Nm^3). Our HPWS designed from conventional rules of chemical and process engineering can be convenient for farm biogas upgrading at flows of biogas beyond 50 Nm^3/h and be sufficient to provide methane enrichment (77%) useful for fuel combustion engines (Saidi et al. [14]).

We show also that conventional approach of HTU and NTU are relevant to predict the behavior efficiency of absorption under different operating conditions of gas and liquid flows.

6. Conclusion

This work allows us to conclude on several critical points regarding the design of High Pressure Water Scrubbing (HPWS) for farm biogas upgrading.

The authors demonstrated that an efficient HPWS designed from conventional rules of chemical and process engineering can be convenient for farm biogas upgrading at flows of biogas beyond 50 Nm^3/h. The designed HPWS has been tested on a real farm with biogas product from biogas plant. Forty experiments have been conducted at the farm scale varying the operating parameters as gas and liquid flows, pressure and temperature.

As an example, we show at the farm scale, that upgrading biogas up to 77% (Q_G=40.7 Nm^3/h and Q_L=8.243m^3/h and P=7.924 bar and T=285K) is possible with good absorption efficiency (57.5%) and high methane recovery ratio (94%) and low power consumption (0.26 kWh/Nm^3).

In terms of operation, water used in the process was successfully recycled thanks to the innovative use of a static mixer. Also, physical entrainment of bubble biogas was avoided thanks to an enlargement of the bottom of the column.

We show also that conventional approach of HTU and NTU are relevant to predict the behavior efficiency of absorption under different operating conditions of gas and liquid flows; from the model, it is possible to select an optimal condition of work for high absorption rate and high recovery methane with low power consumption.

The study revealed also that some differences between experimental and theoretical results exists. They can be due to a residual concentration of CO_2 into recycled water which is unknown and not considered by the model.

Considering the power involved in the process, this work showed that the absorption by HPWS with regenerated water process and cooling system needs 0.25 kWh/Nm^3 of raw biogas to be treated, which is a very good energy demand for upgrading systems useful for flow range of biogas produced on farms and for fuel combustion engines

production.

Acknowledgements

This research was supported by the regional funds for innovation and by ADEME (Agence de l'environnement et de la maitrise de l'énergie). All experiments were performed at the farm of Christophe Canezin, Vic Fezensac, Gers (France). Aria Innovent provided the main operational and material support. LISBP (Ingénierie des Systèmes Biologiques et des Procédés) provided analysis equipment and a scientific support.

Bibliography

[1] J. B. Holm-Nielsen, T. A. Seadi, and P. Oleskowicz-Popiel, "The future of anaerobic digestion and biogas utilization," *Bioresour. Technol.*, vol. 100, no. 22, pp. 5478–5484, 2009.

[2] K. J. McNulty, "Effective design for absorption and stripping," *Chem. Eng.*, vol. 101, no. 11, pp. 92–100, 1994.

[3] F. Bauer, D. Tamm, C. Hulteberg, and T. Persson, "Biogas upgrading – Review of commercial technologies," vol. 2013:270, 2013.

[4] E. Ryckebosch, M. Drouillon, and H. Vervaeren, "Techniques for transformation of biogas to biomethane," *Biomass Bioenergy*, vol. 35, no. 5, pp. 1633–1645, 2011.

[5] M. Poschl, S. Ward, and P. Owende, "Evaluation of energy efficiency of various biogas production and utilization pathways," *Appl. Energy*, vol. 87, no. 11, pp. 3305–3321, 2010.

[6] K. Starr, X. Gabarrell, G. Villalba, L. Talens, and L. Lombardi, "Life cycle assessment of biogas upgrading technologies," *Waste Manag.*, vol. 32, no. 5, pp. 991–999, 2012.

[7] K. A. and R. Nielsen, *Gas purification*. USA : Gulf publishing Company, 1997.

[8] A. J. White, D. W. Kirk, and J. W. Graydon, "Analysis of small-scale biogas utilization systems on Ontario cattle farms," *Renew. Energy*, vol. 36, no. 3, pp. 1019–1025, 2011.

[9] J. Läntelä, S. Rasi, J. Lehtinen, and J. Rintala, "Landfill gas upgrading with pilot-scale water scrubber: Performance assessment with absorption water recycling," *Appl. Energy*, vol. 92, no. 0, pp. 307–314, 2012.

[10] S. Rasi, J. Läntelä, and J. Rintala, "Upgrading landfill gas using a high pressure water absorption process," *Fuel*, vol. 115, no. 0, pp. 539–543, 2014.

[11] S. Rasi, "Biogas Composition and upgrading to biomethane," 2010.

[12] R. Chandra, V. K. Vijay, and P. M. V. Subbarao, "Vehicular Quality Biomethane Production from Biogas by Using an Automated Water Scrubbing System," *ISRN Renew. Energy*, no. 0, p. 6, 2012.

[13] M. Persson, "Evaluation of upgrading techniques for biogas," *Rep. SGC*, vol. 142, 2003.

[14] A. Saidi, C. Trinkl, F. Conti, M. Goldbrunner, J. Karl, "Partially upgraded biogas - Potential for decentralized utilization in agricultural machinery", 2018, Chem. Eng. Technol. 10.1002/ceat.2018001000.

[15] G. Hébrard, D. Benizri, and N. Dietrich, "Dispositif de séparation de constituants gazeux

contenus dans un mélange gazeux et son utilisation pour la séparation de méthane et de dioxyde de carbone," FR1451934, 2014.
[16] G. Hébrard, "Dispositif de récupération de dioxyde de carbone à partir de biogaz," FR1152055, 2011.
[17] H. Sawitowski, *Chem Eng Sci USA*, vol. 6, pp. 138–140, 1957.
[18] M. Roustan, *Tranferts gaz-liquide dans les procédés de traitement des eaux et des effluents gazeux*. Tec&Doc edition, 2003.
[19] W. G. Whitman, "The two film theory of gas absorption," *Int. J. Heat Mass Transf.*, vol. 5, no. 5, pp. 429–433, 1962.
[20] H. T. Onda K. and Y. Okumoto, *J Chem Eng Jpn.*, vol. 1, pp. 56–62, 1968.
[21] E. Treybal Robert, *Mass-transfer operations*. McGraw-Hill Book Company, 1981.
[22] A. Heyouni, "Hydrodynamique et transfert de matière gaz-liquide dans les mélangeurs statiques," thèse INSA de Toulouse, 2002.
[23] T. U. Fischer and F. A. Streiff, "New fundamentals for liquid-liquid dispersion using static mixer," *Récent Prog. En Génie Procédés*, vol. 11, no. 51, pp. 307–314, 1997.
[24] Zhou, "Design guide for motionless mixers as gas-liquid reactor," 1992.
[25] P. Andreussi, A. Paglianti, and F. S. Silva, "Dispersed Bubble Flow in Horizontal Pipes," *Chem Eng Sci*, vol. 54, pp. 1101–1107, 1999.
[26] C. R. Wilke and P. Chang, *Appl Ind Ch Eng*, pp. 1–264, 1955.
[27] P. Devos, "Un mélangeur statique aux applications multiples," *Inf. Chim.*, no. 109, pp. 109–123, 1972.
[28] I. Calmel and J. Magnaudet, "Transfert de masse à l'interface d'un film turbulent libre ou cisaillé," *Rev Gen Therm*, vol. 37, pp. 769–780, 1998.
[29] S. Mao, Z. Duan, D. Zhang, L. Shi, Y. Chen, and J. Li, "Thermodynamic modeling of binary CH4–H2O fluid inclusions," *Geochim. Cosmochim. Acta*, vol. 75, no. 20, pp. 5892–5902, 2011.
[30] Z. Duan and R. Sun, "An improved model calculating {CO2} solubility in pure water and aqueous NaCl solutions from 273 to 533 K and from 0 to 2000 bar," *Chem. Geol.*, vol. 193, no. 3–4, pp. 257–271, 2003.
[31] G. H. S. Sherwood T.K. and F. A. L. Holloway, *Ind Eng Chem USA 30*, pp. 765–769, 1938.
[32] F. H. Lobo W.E. L. Friend and F. Zenz, *Trans Am Inst Chem Engrs USA*, vol. 41, pp. 1693–1710, 1945.

Appendix A. Nomenclature

Latin Letters

a^0 Real wet surface offered by the packing $[m^2.m^{-3}]$

a^* Geometrical surface offered by the packing $[m^2.m^{-3}]$

A Absorption rate

C Liquid concentration $[mol.m^{-3}]$

C^* Liquid concentration at saturation according to Henry's law in diluted solution and at operational conditions $[mol.m^{-3}]$

d Diameter [m]
Dc Column diameter [m]
D_i Diffusion coefficient of the component i [$m^2.s^{-1}$]

E_G Efficiency of gas absorption

F Packing factor [m^2/m^3]

g Gravity constant [$m.s^{-2}$]
G Molar flow [$mol.s^{-1}$]
G_M Gas mass fl w [$kg.s^{-1}$]
H Henry constant [Pa]
HTU_{OG} Height of a transfer unit [m]
k^0 Film convective transfer coefficient [$mol.m^{-2}.s^{-1}$]
K Global convective mass transfer coefficient [$m.s^{-1}$]

K_La Volumetric convective mass transfer coefficient [s^{-1}]

K_{Lpip} Global convective mass transfer coefficient in a stratified pipe [$m.s^{-1}$]

L Solvent molar flow [$mol.s^{-1}$]

L_M Solvent mass flow [$kg.s^{-1}$]
m Sharing coefficient

M Molar mass [$g.mol^{-1}$]
NTU_{OG} Number of transfer unit
P Pressure [Pa]
P_{dis} Dissipated power [W]
Q Volumetric flow [$Nm^3.s^{-1}$]
R Perfect gas constant
R_{CH_4} Rate of upgraded methane
S Gas/liquid interface in a stratified flow [m^2]

T Temperature [K]
U Velocity [$m.s^{-1}$]
V Volume [m^3]
x Liquid molar rate [$mol.mol^{-1}$]
X liquid molar rate relative to non-transferring components [$mol.mol^{-1}$]

y Gaseous molar rate [$mol.mol^{-1}$]
Y Gaseous molar rate relative to non-transferring components [$mol.mol^{-1}$]

Z Column height [m]

Greek Letters

α Parameter for calculating bubble Sauter diameter

Δ I variation of the parameter I

ϵ_i volume rate of phase i

Ω Column cross section [m^2]

ρ Density [$kg.m^{-3}$]
τ Residence time [s]

σ Surface tension [$N.m^{-1}$]
Σ liquid mass content of the static mixer [kg]

μ Dynamic viscosity [Pa.s]

Subscripts

b - Related to bubble

bottom - Related to the bottom column

bs - Related to the Sauter equivalent bubble

c - Related to the column
CH_4 - Related to CH_4
CO_2 - Related to CO_2
crit - At critical condition
Flood - At flooding condition

G - Related to the gas phase

i - Related to the component i

in - Related to the inlet of the process

inert - Related to inert component

L - Related to the solvent phase

mean - Mean of the related parameter

O_2 - Related to O_2

out - Related to the outlet of the process

p - Related to the packing

SM - Related to the static mixer

Dimensionless numbers

Re_L is the Reynolds number for the liquid phase

$$Re_L = \frac{\rho_L \cdot U_L \cdot d_p}{\mu_L}$$

Sc_L is the Schmidt number

$$Sc_L = \frac{\mu_L}{\rho_L \cdot D_L}$$

Sh_G is the Sherwood number

$$Sh_G = \frac{d_{eq}}{D_G}$$

Ga_L is the Galilei number

$$Ga_L = \frac{g \cdot {d_p}^3 \cdot {\rho_L}^2}{{\mu_L}^2}$$

We_L is the Weber number

$$We_L = \frac{d_p \cdot {L_M}^2}{\rho_L \cdot \sigma_L}$$

Appendix B. Literature correlations

Absorption flows calculation

Ordinate Y_{Flood} is given by reading on a graph produced by Sherwood [31] and refitted by Lobo et al. [32], or using the correlations suggested by Sawitowski [17].

$$Y_{FLOOD} = 0.684 \cdot \exp(-3.61 \cdot {X_{FLOOD}}^{0,286})$$

Absorption mass transfer calculation

a^* [m^2/m^3] is the geometrical surface offered by the packing and a^0 is the real wetted surface during operation. This surface can be evaluated with the correlation of Onda [20]:

$$\frac{a^0}{a^*} = 1 - \exp(-1.45 \cdot \left(\frac{\sigma_p}{\sigma_L}\right)^{0.75} \cdot (a^* \cdot d_p)^{-0.35} \cdot {Ga_L}^{0.05} \cdot {We_L}^{0.2}$$